

# In-beam $\gamma$ -ray spectroscopy at the proton dripline: $^{23}\text{Al}$

A. Gade<sup>a,b</sup> P. Adrich<sup>a</sup> D. Bazin<sup>a</sup> M. D. Bowen<sup>a,b</sup>  
 B. A. Brown<sup>a,b</sup> C. M. Campbell<sup>a,b</sup> J. M. Cook<sup>a,b</sup>  
 T. Glasmacher<sup>a,b</sup> K. Hosier<sup>c</sup> S. McDaniel<sup>a,b</sup> D. McGlinchery<sup>c</sup>  
 A. Obertelli<sup>a</sup> L. A. Riley<sup>c</sup> K. Siwek<sup>a,b</sup> J. A. Tostevin<sup>d</sup>  
 D. Weisshaar<sup>a</sup>

<sup>a</sup>*National Superconducting Cyclotron Laboratory, East Lansing, MI 48824, USA*

<sup>b</sup>*Department of Physics & Astronomy, Michigan State University, East Lansing, MI 48824, USA*

<sup>c</sup>*Department of Physics and Astronomy, Ursinus College, Collegeville, PA 19426, USA*

<sup>d</sup>*Department of Physics, Faculty of Engineering and Physical Sciences, University of Surrey, Guildford, Surrey GU2 7XH, United Kingdom*

---

## Abstract

We report on the first in-beam  $\gamma$ -ray spectroscopy of  $^{23}\text{Al}$  using two different reactions at intermediate beam energies: inelastic scattering off  $^9\text{Be}$  and heavy-ion induced one-proton pickup,  $^9\text{Be}(^{22}\text{Mg}, ^{23}\text{Al}+\gamma)\text{X}$ , at 75.1 MeV/nucleon. A  $\gamma$ -ray transition at 1616(8) keV – exceeding the proton separation energy by 1494 keV – was observed in both reactions. From shell model and proton decay calculations we argue that this  $\gamma$ -ray decay proceeds from the core-excited  $7/2^+$  state to the  $5/2^+$  ground state of  $^{23}\text{Al}$ . The proposed nature of this state,  $[^{22}\text{Mg}(2_1^+) \otimes \pi d_{5/2}]_{7/2^+}$ , is consistent with the presence of a  $\gamma$ -branch and with the population of this state in the two reactions.

*Key words:*

*PACS:* 23.20.Lv, 25.60.-t, 21.60.Cs, 27.30.+t

---

Since its discovery in 1969 [1], the neutron-deficient nucleus  $^{23}\text{Al}$  has attracted much attention.  $^{23}\text{Al}$  is four neutrons removed from stable  $^{27}\text{Al}$  and is the last proton-bound, odd-mass aluminum isotope known to exist. The low proton separation energy of  $S_p = 122(19)$  keV [2] made  $^{23}\text{Al}$  a candidate for a proton halo system. From the measurement of an enhanced reaction cross section,  $^{23}\text{Al}$  was indeed proposed to have a proton-halo structure with a  $J^\pi = 1/2^+$

assignment suggested for the spin and parity of the ground state [3,4]. However, a  $\beta$ NMR measurement clearly showed that the spin and the parity of the  $^{23}\text{Al}$  ground state are  $J^\pi = 5/2^+$  [5], in agreement with the mirror nucleus  $^{23}\text{Ne}$ . Excited states of  $^{23}\text{Al}$  have been studied in  $^{24}\text{Mg}(^7\text{Li}, ^8\text{He})^{23}\text{Al}$  reactions [7,6], in  $\beta$ -delayed proton decay [8], in Coulomb breakup [9] and most recently in  $^{22}\text{Mg} + p$  resonant proton scattering [10]. None of these prior experiments was sensitive to  $\gamma$ -ray transitions in  $^{23}\text{Al}$ . In the present paper we report on the first in-beam  $\gamma$ -ray spectroscopy study of  $^{23}\text{Al}$ . Two complementary reactions were used to excite  $^{23}\text{Al}$ : inelastic scattering off a  $^9\text{Be}$  target and the heavy-ion induced one-proton pickup reaction,  $^9\text{Be}(^{22}\text{Mg}, ^{23}\text{Al}+\gamma)\text{X}$ .

Both measurements were performed with an exotic cocktail beam composed of 32%  $^{22}\text{Mg}$  and 3%  $^{23}\text{Al}$ . This secondary beam was produced in-flight by fragmentation of a 150 MeV/nucleon  $^{36}\text{Ar}$  primary beam delivered by the Coupled Cyclotron Facility at NSCL on the campus of Michigan State University. The primary  $^9\text{Be}$  production target (893 mg/cm<sup>2</sup> thick) was located at the mid-acceptance target position of the A1900 fragment separator [11]; an achromatic aluminum wedge degrader of 300 mg/cm<sup>2</sup> thickness and momentum slits at the dispersive image of the separator were used to select the secondary beam. As the available total secondary beam intensity exceeded various rate limitations (timing detectors before the reaction target and data acquisition), the slits were restricted to  $\Delta p/p=0.5\%$  total momentum acceptance for the secondary beam resulting in the very clean particle identification discussed later.

The  $^9\text{Be}(^{23}\text{Al}, ^{23}\text{Al}+\gamma)^9\text{Be}$  inelastic scattering and the  $^9\text{Be}(^{22}\text{Mg}, ^{23}\text{Al}+\gamma)\text{X}$  one-proton pickup reaction were induced by a 188(4) mg/cm<sup>2</sup>  $^9\text{Be}$  target placed at the target position of the S800 spectrograph [12]. The reaction target was surrounded by SeGA [13] in its “classic” configuration with nine and seven detectors, respectively, at central angles of 90° and 37° with respect to the beam axis. The SeGA high-purity germanium detectors are 32-fold segmented and allow for an event-by-event Doppler reconstruction of the  $\gamma$ -rays emitted in-flight by the reacted nuclei. The emission angle that enters the Doppler reconstruction is determined from the location of the segment with the largest energy deposition relative to the target.

Event-by-event particle identification was performed in all entrance and exit channels with timing detectors before the reaction target and with the focal-plane detection system [14] of the S800 spectrograph. The time-of-flight difference measured between the two plastic scintillators located before the reaction target allowed for an unambiguous identification of all constituents of the incoming cocktail beam (see Fig. 2 of [15] and Fig. 1 of [16]). The reaction residues emerging from the  $^9\text{Be}$  target were identified via their time-of-flight measured by plastic scintillators and their energy loss determined with the S800 ion chamber. A software gate on the incoming beam then allowed the

selection of only those reaction residues induced by the projectile of interest (see also refs. [15,16]).

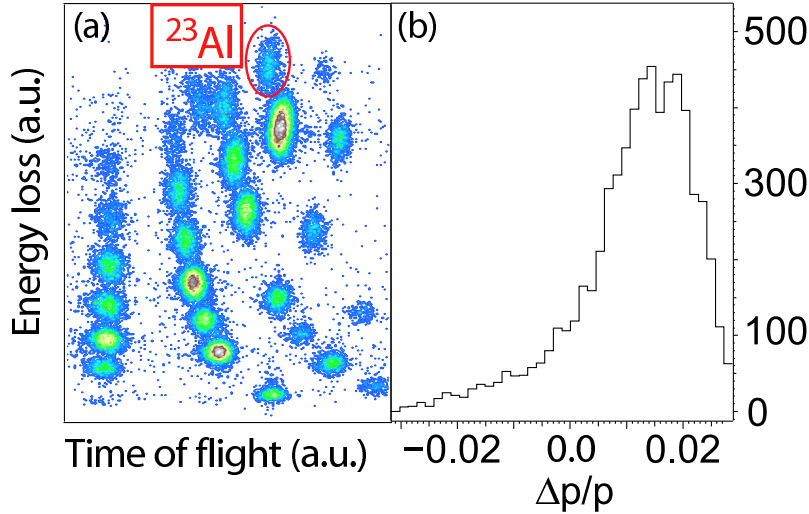


Fig. 1. Left: Identification spectrum – energy loss vs. time of flight – of  $^{23}\text{Al}$  produced in the one-proton pickup of  $^{22}\text{Mg}$  projectiles from the  $^9\text{Be}$  target. Right: Parallel momentum distribution of  $^{23}\text{Al}$  (relative to  $p = 7.990 \text{ GeV}/c$ ); shown is the full momentum acceptance of the spectrograph.

Fig. 1(a) shows the particle identification spectrum – energy loss vs. time-of-flight – for the spectrograph setting that was optimized on the one-proton pickup channel. The particle identification spectrum only contains reaction products from  $^{22}\text{Mg}$ . The one-proton pickup residue  $^{23}\text{Al}$  can be clearly separated from the fragmentation products that enter the S800 focal plane as well. Fig. 2(a) shows the event-by-event Doppler reconstructed  $\gamma$ -ray spectrum in coincidence with  $^{23}\text{Al}$  produced in the one-proton pickup reaction. A photopeak at 1614(9) keV is clearly visible and marks a  $\gamma$ -ray transition in  $^{23}\text{Al}$ .

Fig. 3(a) shows the particle identification of the inelastically scattered  $^{23}\text{Al}$ . The spectrograph setting was optimized on the one-neutron knockout reaction  $^9\text{Be}(^{24}\text{Si},^{23}\text{Si})\text{X}$  which is discussed in [16]. For a single-neutron knockout setting in this mass region, the magnetic rigidity of the spectrograph is more than 4% lower than for a setting centered on the projectiles passing through the target. Thus only the low-momentum tail of the scattered  $^{23}\text{Al}$  projectiles can enter the spectrograph as displayed in Fig. 3(b). In coincidence with these scattered  $^{23}\text{Al}$  nuclei, that must have been subject to a significant momentum transfer, to be found in the outmost low-momentum tail of the distribution, a  $\gamma$ -ray transition was observed at 1618(8) keV (Fig. 2(b)).

The observed  $\gamma$ -ray energy is consistent for the two measurements and implies an excited state at 1616(8) keV in  $^{23}\text{Al}$ , 1494 keV above the proton separation energy. This state has a significant  $\gamma$ -ray branch to the proton-bound ground

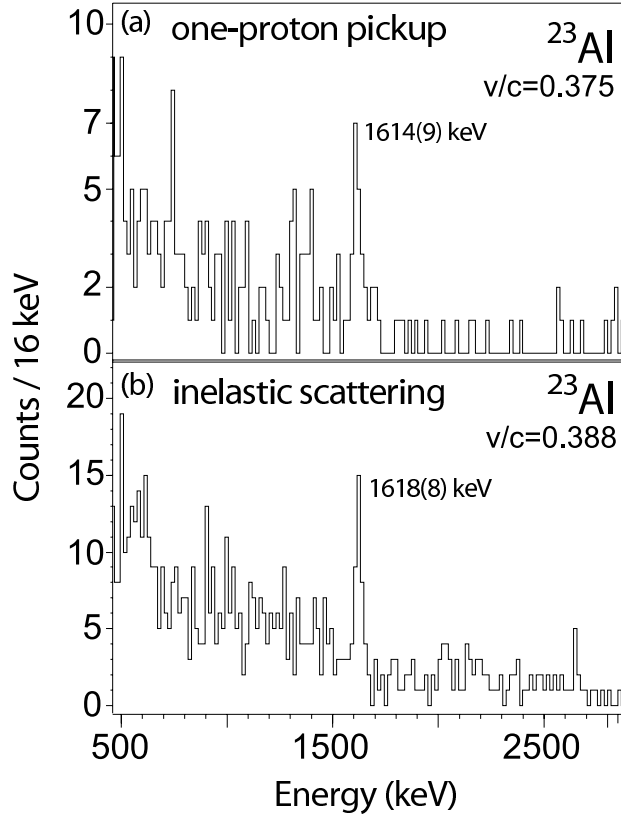


Fig. 2. Doppler-reconstructed  $\gamma$ -ray spectrum measured in coincidence with  $^{23}\text{Al}$  reaction residues produced in one-proton pickup (upper panel) and inelastic scattering (lower panel). The energy uncertainty is dominated by the uncertainty in the target position which is systematic and common for both measurements.

state. If this  $\gamma$ -ray transition were to originate from an even higher excited state it would either populate a proton-unbound excited state and could not have been observed here as a coincidence with  $^{23}\text{Al}$  is required or would feed an excited state that also has a significant  $\gamma$ -ray decay branch which then should have been detected as well.

All excited states of  $^{23}\text{Al}$  are reported to decay to 100% by proton emission, including the first excited state,  $E(1/2^+) = 550(20)$  keV, with an estimated branching of  $\Gamma_p/\Gamma_\gamma \sim 10^8$  [6,9,17]. Figure 4 compares the level schemes of the mirror nuclei  $^{23}\text{Al}$  and  $^{23}\text{Ne}$  below 2.3 MeV excitation energy. We tentatively assign spin and parity  $J^\pi = (7/2^+)$  to the excited state at 1616(8) keV observed in the present work. There is a one-to-one correspondence for the states below 2.3 MeV. The energy difference of the  $1/2^+$  first excited state can be explained by the Thomas-Ehrman shift [18] which influences  $\ell = 0$  orbits the most. In the following we discuss the structure of the proposed  $7/2^+$  state, in particular the occurrence of a significant  $\gamma$ -ray branch, within the USD shell model and argue the consistency of this assignment with the reaction mechanisms that led to its observation.

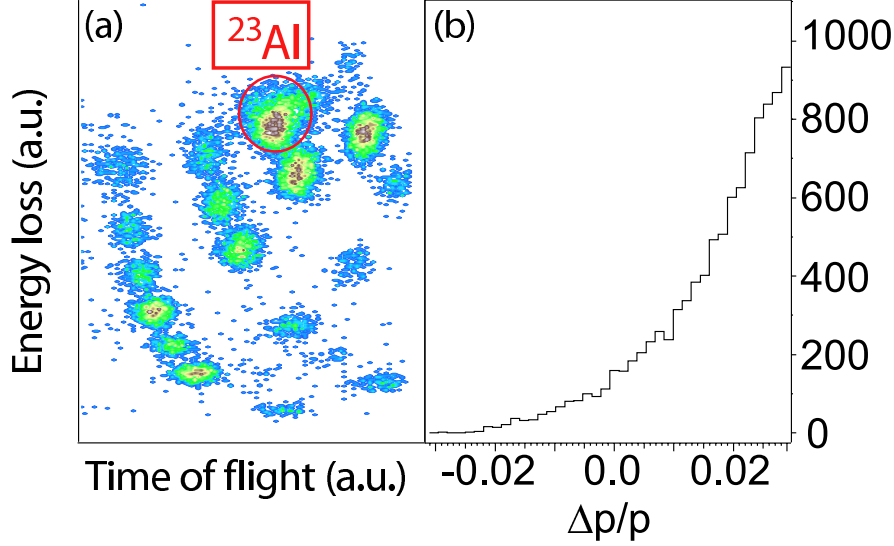


Fig. 3. Left: Identification spectrum – energy loss vs. time of flight – of the (in)elastically scattered  $^{23}\text{Al}$  nuclei. The spectrograph magnetic rigidity was centered on the one-neutron removal products from  $^{24}\text{Si}$ . Right: Parallel momentum distribution of the scattered  $^{23}\text{Al}$  (relative to  $p = 8.339 \text{ GeV}/c$ ). Due to the magnetic rigidity setting optimized on reaction residues with one neutron less than the projectile, only the low-momentum tail of scattered  $^{23}\text{Al}$  enters the focal plane.

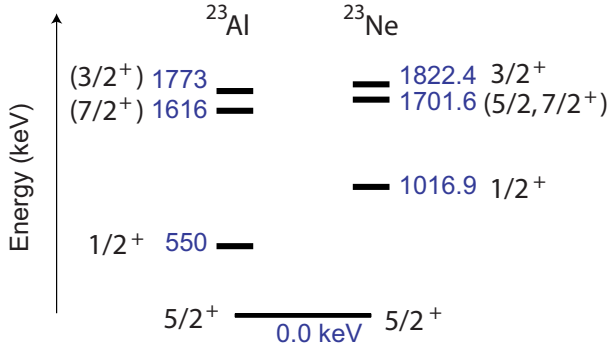


Fig. 4. Low lying level schemes of the mirror nuclei  $^{23}\text{Al}$  and  $^{23}\text{Ne}$  below 2.3 MeV excitation energy. The large difference in the energy of the  $1/2^+$  state can be attributed to the Thomas-Ehrman shift [18] which is strongest for states with orbital angular momentum  $\ell = 0$ . The state at 1616(8) keV in  $^{23}\text{Al}$  is reported for the first time.

Shell-model calculations for the energies, spectroscopic factors and electromagnetic matrix elements were carried out with the USDB effective interaction (results with USDA were similar) [19]. The calculated half-life of the  $7/2^+$  state,  $T_{1/2} = 23 \text{ fs}$ , corresponds to a  $\gamma$  width of  $\Gamma_\gamma = 0.020 \text{ eV}$ . The spectroscopic factor for the  $d_{5/2}$  orbit connecting the  $^{23}\text{Al}$ ,  $J^\pi = 7/2^+$  and  $^{22}\text{Mg}$ ,  $J^\pi = 2^+$  levels is large indicating a dominance of the  $[^{22}\text{Mg}(2_1^+) \otimes d_{5/2}]_{7/2^+}$  configuration in the  $^{22}\text{Mg}$  wave function. From the energetics summarized in Fig. 5, it follows that the  $Q$ -value for this decay is  $Q_p = 244(21) \text{ keV}$ .

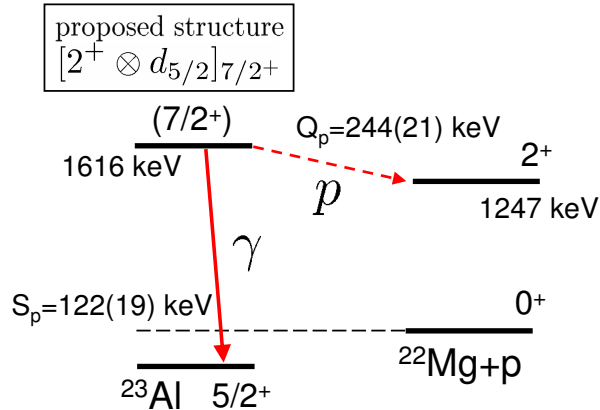


Fig. 5. Proposed decay scheme of the  $7/2^+$  core-coupled state at 1616(8) keV in  $^{23}\text{Al}$ . The state at 1616(8) keV in  $^{23}\text{Al}$  was observed for the first time in the present experiment.

To quantify the proton decay of the  $7/2^+$  state, the proton scattering cross section was calculated for  $\ell = 2$  at  $Q_p = 244$  keV with a Woods-Saxon potential and the resulting resonance width was used as the single-particle proton decay width,  $\Gamma_p^{sp} = 0.0024$  eV. With the value  $S = 0.46$  for the  $7/2^+$  to  $[^{22}\text{Mg}(2_1^+) \otimes d_{5/2}]$  spectroscopic factor, from the USDB shell-model calculations, this yields a proton decay width of  $\Gamma_p = S \times \Gamma_p^{sp} = 0.0011$  eV for the decay of the  $7/2^+$  state of  $^{23}\text{Al}$  to the first excited  $2^+$  state of  $^{22}\text{Mg}$ . In conclusion, the proposed structure of the  $7/2^+$  state, together with the energetics of the proton decay (see Fig. 5), results in  $\Gamma_\gamma/\Gamma_p \sim 20$  consistent with the observation of the  $\gamma$ -decay of this state. We note that proton detection was not possible with our experimental setup. Furthermore,  $^{22}\text{Mg}$  residues populated by the proton decays of excited states of  $^{23}\text{Al}$  could not be distinguished from  $^{22}\text{Mg}$  produced by the fragmentation of the  $^{23}\text{Al}$  projectiles, for example. Proton decay to the  $^{22}\text{Mg}$  ground state could proceed by  $\ell = 4$ . The single-particle proton decay width from the potential scattering calculations for  $\ell = 4$  with  $Q_p = 1.49$  MeV is 10 eV. If we assume that the proton width is approximately less than or equal to the gamma width then  $S \leq 0.002$  for the  $g_{7/2}$  spectroscopic factor. Thus, the  $g$ -orbital admixture into the  $sd$  model space is very small.

In our experiment, the state at 1616 keV was excited in the inelastic scattering of  $^{23}\text{Al}$  from a  $^9\text{Be}$  target. In odd- $A$  nuclei, core-coupled states are most likely excited in inelastic scattering processes or Coulomb excitation. This is consistent with the spin and parity assignment of  $J^\pi = 7/2^+$  for this state and the proposed structure discussed above.

However, our analysis was restricted to scattering events with a large momentum loss, as only the low-momentum tails of the scattered projectiles – including  $^{23}\text{Al}$  – were within the acceptance of the S800 spectrograph. To probe the nature of the states excited in these scattering events, another con-

stituent of the cocktail beam,  $^{22}\text{Mg}$ , was studied under identical conditions. In the same reaction setting where the 1616 keV  $\gamma$ -ray was measured in coincidence with the low-momentum tail of the  $^{23}\text{Al}$  projectile distribution passing through the target, the low-momentum tail of the  $^{22}\text{Mg}$  projectiles within the same cocktail beam entered the focal plane as well. The event-by-event Doppler reconstructed  $\gamma$ -ray spectrum in coincidence with these inelastically scattered  $^{22}\text{Mg}$  projectiles is shown in Fig. 6. The photopeaks of the  $2_1^+ \rightarrow 0_1^+$  and  $4_1^+ \rightarrow 2_1^+$   $\gamma$ -ray transitions are clearly visible. The intensities show that, predominantly, the  $2_1^+$  state of  $^{22}\text{Mg}$  is excited in the inelastic scattering of  $^{22}\text{Mg}$  projectiles from the  $^9\text{Be}$  target. This is again consistent with the proposed structure of [ $^{22}\text{Mg}(2_1^+) \otimes d_{5/2}$ ] for the 1616 keV state excited in the inelastic scattering of  $^{23}\text{Al}$ .

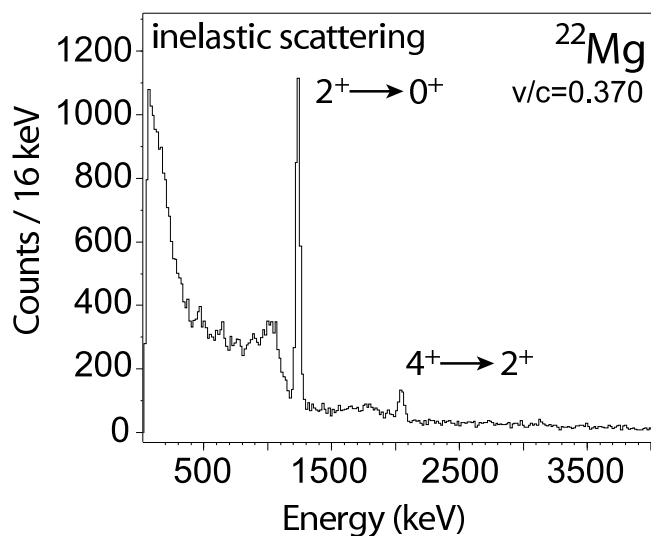


Fig. 6. Doppler-reconstructed  $\gamma$ -ray spectrum obtained from the inelastic scattering of  $^9\text{Be} + ^{22}\text{Mg}$  in a setting where only the low-momentum tail of the scattered  $^{22}\text{Mg}$  projectile distribution entered the focal plane. The first  $2^+$  and  $4^+$  states are populated.

The proposed ( $7/2^+$ ) excited state in  $^{23}\text{Al}$  was also populated in the one-proton pickup reaction  $^9\text{Be}(^{22}\text{Mg}, ^{23}\text{Al} + \gamma)\text{X}$ . The  $^{22}\text{Mg}$  energy was 75.1 MeV/nucleon at mid-target. The potential of using inverse-kinematics one-proton pickup reactions with fast exotic beams for spectroscopy has recently been investigated at the NSCL with the reaction  $^9\text{Be}(^{20}\text{Ne}, ^{21}\text{Na} + \gamma)\text{X}$  [21]. In that case, the pattern of the observed population of  $^{21}\text{Na}$  single-proton states was found to be consistent with distorted wave transfer reaction calculations and shell-model theory. There also, a core-coupled  $7/2^+$  state was observed in  $^{21}\text{Na}$ , with a partial cross section of 0.20(5) mb from an inclusive cross section of 1.85(12) mb [21]. While unobserved feeding from higher-lying states could not be excluded, the direct population of this state with a complex structure would indicate the presence of higher-order processes, as for example the pickup onto  $^{20}\text{Ne}$  in its  $2_1^+$  excited state.

For the one-proton pickup to  $^{23}\text{Al}$ , the subject of the present paper, an inclusive cross section of  $\sigma = 0.54(5)$  mb was measured for the  $^9\text{Be}(^{22}\text{Mg}, ^{23}\text{Al})X$  reaction. From the  $\gamma$ -ray intensity, a partial cross section of  $\sigma(7/2^+) \geq 0.07(2)$  mb was determined with  $\sigma(7/2^+) = 0.07(2)$  mb for  $\Gamma_p = 0$ <sup>1</sup>. The populations of the core-excited  $7/2^+$  states in  $^{21}\text{Na}$  [21] and  $^{23}\text{Al}$  (present work), at about 11% and 14%, respectively, are consistent for the two measurements and suggestive of the proposed assignment in  $^{23}\text{Al}$ . The low-momentum tail of the  $^{23}\text{Al}$  one-proton pickup residue distribution (evident in Fig. 1(b)) is also indicative of the presence of multi-step or unbound  $^8\text{Li}$  final state contributions in the reaction process. The population of other (single-proton) states in  $^{23}\text{Al}$ , other than the  $5/2^+$  ground and  $7/2^+$  excited state could not be observed as these states decay by proton emission [17].

A reaction analysis of the present  $^9\text{Be}(^{22}\text{Mg}, ^{23}\text{Al})X$  proton pickup data was performed within the finite-range, post form of the coupled channels Born approximation (CCBA) treating direct multi-step reactions via transfer and inelastic channels using the direct reactions code FRESKO [22]. Single-step  $1d_{5/2}$  proton transfer onto  $^{22}\text{Mg}(J^\pi)$  core states was assumed (from  $^9\text{Be}$ ) according to the coupling scheme shown in Figure 7. It was also assumed (see Ref. [21]) that the final states were two-body. Thus the basic proton pickup mechanism is computed as  $^{22}\text{Mg}(^9\text{Be}, ^8\text{Li}(I^+))^{23}\text{Al}(j^\pi)$  leading to the  $I^\pi = 1^+, 2^+$  and  $3^+$  states of  $^8\text{Li}$  at 75.1 MeV per nucleon incident energy. The (absorptive) nuclear interactions were calculated, as in recent nucleon knockout reaction studies, by double folding the neutron and proton densities of  $^{22}\text{Mg}$  (from Hartree-Fock calculations) and of  $^9\text{Be}$  (assumed a Gaussian with rms radius of 2.36 fm) with an effective nucleon-nucleon (NN) interaction [23]. The  $^{22}\text{Mg}$  was allowed to inelastically excite by deforming the entrance channel distorting potential, taking a deformation length  $\delta_2 = 1.95$  fm. This corresponds to an assumed  $^{22}\text{Mg}$  mass  $\beta_2$  value of 0.58; this is taken from the charge  $\beta_2$  value 0.58(11) of Ref. [24]. The (light) target-like vertices,  $[^8\text{Li}(I^+) \otimes \Phi_j]_{3/2^-}$ , were treated as in Ref. [21], making use of the Variational Monte Carlo (VMC) overlaps and spectroscopic amplitudes [25].

The required proton-core projectile overlaps,  $[^{22}\text{Mg}(J^\pi) \otimes \pi 1d_{5/2}]_j$ , and their spectroscopic amplitudes were guided by the USDB shell model calculations. As is noted in Fig. 7 there are interfering spectroscopic amplitudes  $\alpha$  and  $\beta$  for population of the  $^{23}\text{Al}(\text{gs})$  via the  $[^{22}\text{Mg}(0^+) \otimes \pi 1d_{5/2}]_{5/2}$  and  $[^{22}\text{Mg}(2^+) \otimes \pi 1d_{5/2}]_{5/2}$  transfers, respectively. The  $^{23}\text{Al}(7/2^+)$  state is populated by  $[^{22}\text{Mg}(2^+) \otimes \pi 1d_{5/2}]_{7/2}$ . The USDB shell model spectroscopic factors of these overlaps are  $S=0.33, 0.84$  and  $0.46$ , respectively. The associated  $\pi 1d_{5/2}$  single particle states

<sup>1</sup> We note that our experiment was not designed to detect protons or to separate  $^{22}\text{Mg}$  produced by the proton decay of  $^{23}\text{Al}$  from  $^{22}\text{Mg}$  produced in projectile fragmentation and thus the cross section for the population of the  $7/2^+$  determined from  $\gamma$ -ray spectroscopy is a lower limit if  $\Gamma_p \neq 0$ .



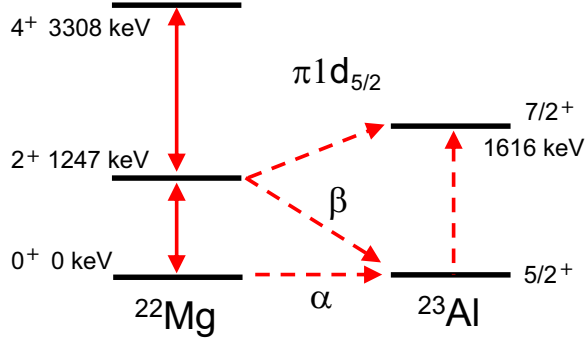


Fig. 7. Schematic of the channel coupling scheme for the coupled channels Born approximation calculations of the  $^{22}\text{Mg}(^9\text{Be}, ^8\text{Li})^{23}\text{Al}(j^\pi)$  reaction.

were calculated in real Woods-Saxon potential wells with radius and diffuseness parameters  $r_0 = 1.25$  fm and  $a_0 = 0.7$  fm and a spin-orbit interaction of strength 6 MeV with the same geometry parameters. The bound  $\pi 1d_{5/2}$  configurations used the physical separation energies. The very narrow resonant  $\pi 1d_{5/2}$  state, relevant to the  $7/2^+$  transition with  $S_p = -244$  keV, was described by a bound proton state with separation energy of  $S_p = +5$  keV.

The calculated yields, inclusive with respect to the three  $^8\text{Li}(I^+)$  final state contributions, were as follows. The cross section for direct population of the  $^{23}\text{Al}(7/2^+)$  state is 0.022 mb, underproducing the measured yield of 0.07(2) mb. The calculations were also sensitive to the relative phase of the spectroscopic amplitudes  $\alpha$  and  $\beta$  that feed the  $^{23}\text{Al}(\text{gs})$ , Fig. 7. The shell-model calculations for the spectroscopic amplitudes together with the electromagnetic matrix element, predicts that these paths interfere destructively to give  $^{23}\text{Al}(\text{gs})$  and inclusive cross sections of 0.26 and 0.28 mb, the latter to be compared with the experimental value of 0.54(5) mb. Inelastic  $5/2^+ \rightarrow 7/2^+$  (single particle) coupling in  $^{23}\text{Al}$ , shown in Fig. 7, was found to have negligible effect on the calculated  $^{23}\text{Al}(7/2^+)$  yield. We conclude that the *relative* yields of the  $^{23}\text{Al}(5/2^+)$  and  $^{23}\text{Al}(7/2^+)$  are reasonably reproduced by the model calculations. The inclusive cross section is a factor two smaller than that measured. These lower cross sections were not unexpected since we include only the three (lowest)  $^8\text{Li}$  final states with summed spectroscopic factors of 0.97 ( $p_{3/2}$ ) and 0.36 ( $p_{1/2}$ ). Further consideration of strength leading to the  $^8\text{Li}$  continuum is needed to assess the absolute cross sections. As was noted above, the low-momentum tail seen in the  $^{23}\text{Al}$  distribution in Fig. 1 suggests a significant missing dissipative mechanism such as coupling to the  $^8\text{Li}$  continuum.

In summary, the  $\gamma$ -decay of an excited state in  $^{23}\text{Al}$  has been observed for the first time in (i)  $^{23}\text{Al}$  inelastic scattering from  $^9\text{Be}$  and (ii) in the heavy-ion induced one-proton pickup reaction  $^9\text{Be}(^{22}\text{Mg}, ^{23}\text{Al}+\gamma)\text{X}$ . The corresponding excited state at 1616(8) keV lies 1494 keV above the proton separation energy of  $^{23}\text{Al}$ . The presence of the  $\gamma$ -ray decay branch and the population of this state in the two reaction mechanisms is consistent with the state being the

$7/2^+$  core-excited configuration,  $[^{22}\text{Mg}(2_1^+) \otimes d_{5/2}]_{7/2^+}$ , predicted by the shell model to be the second excited state. This picture is also consistent with the relative yields of the ground and  $7/2^+$  states obtained using multi-step, CCBA reaction calculations. We have shown that the proton decay of this state, which will proceed by emission of a proton from the  $d_{5/2}$  orbit to the first  $2^+$  state of  $^{22}\text{Mg}$ , is hindered by the small  $Q$ -value of  $Q_p = 244(21)$  keV. A branching ratio of  $\Gamma_\gamma/\Gamma_p \sim 10$  is estimated from shell model and proton decay calculations.

This work was supported by the National Science Foundation under Grants No. PHY-0606007, PHY-0555366 and PHY-0653323 and by the United Kingdom Science and Technology Facilities Council (STFC) under Grant EP/D003628.

## References

- [1] J. Cerny, R. A. Mendelson, Jr., G. J. Wozniak, J. E. Esterl, and J. C. Hardy, *Phys. Rev. Lett.* 22 (1969) 612.
- [2] G. Audi, A. H. Wapstra and C. Thibault, *Nucl. Phys.* A729 (2003) 337.
- [3] X. Z. Cai, H. Y. Zhang, W. Q. Shen, Z. Z. Ren, J. Feng *et al.*, *Phys. Rev. C* 65 (2002) 024601.
- [4] H. Y. Zhang, W. Q. Shen, Z. Z. Ren, Y. G. Ma, J. G. Chen, X. Z. Cai, C. Zhong, X. F. Zhou, Y. B. Wei, G. L. Ma, and K. Wang, *Nucl. Phys.* A722 (2003) 518c.
- [5] A. Ozawa, K. Matsuta, T. Nagatomo, M. Mihara *et al.*, *Phys. Rev. C* 74 (2006) 021301(R).
- [6] J. A. Caggiano, D. Bazin, W. Benenson, B. Davids, R. Ibbotson *et al.*, *Phys. Rev. C* 64 (2001) 025802.
- [7] M. Wiescher, J. Görres, B. Sherrill, M. Mohar, J. S. Winfield, and B. A. Brown, *Nucl. Phys.* A484 (1988) 90.
- [8] B. Blank, F. Boue, S. Andriamonje, S. Czajkowski, R. Del Moral, J. P. Dufour, A. Fleury, P. Pourre, M. S. Pravikoff, E. Hanelt, N. A. Orr, and K.-H. Schmidt, *Z. Phys. A* 357 (1997) 2467.
- [9] T. Gomi, T. Motobayashi, Y. Ando, N. Aoi, H. Baba *et al.*, *Nucl. Phys.* A758 (2005) 761.
- [10] J. J. He, S. Kubono, T. Teranishi, M. Notani, H. Baba, S. Nishimura, J. Y. Moon, M. Nishimura, H. Iwasaki, Y. Yanagisawa, N. Hokoïwa, M. Kibe, J. H. Lee, S. Kato, Y. Gono, and C. S. Lee, *Phys. Rev. C* 76 (2007) 055802.
- [11] D. J. Morrissey *et al.*, *Nucl. Instrum. Methods in Phys. Res. B* 204 (2003) 90.
- [12] D. Bazin *et al.*, *Nucl. Instrum. Methods in Phys. Res. B* 204 (2003) 629.

- [13] W. F. Mueller *et al.*, Nucl. Instr. and Meth. A 466 (2001) 492.
- [14] J. Yurkon *et al.*, Nucl. Instrum. Methods in Phys. Res. A 422 (1999) 291.
- [15] A. Gade, P. Adrich, D. Bazin, M. D. Bowen, B. A. Brown, C. M. Campbell, J. M. Cook, T. Glasmacher, K. Hosier, S. McDaniel, D. McGlinchery, A. Obertelli, L. A. Riley, K. Siwek, and D. Weisshaar, Phys. Rev. C 76 (2007) 024317.
- [16] A. Gade, P. Adrich, D. Bazin, M. D. Bowen, B. A. Brown, C. M. Campbell, J. M. Cook, T. Glasmacher, K. Hosier, S. McDaniel, D. McGlinchery, A. Obertelli, L. A. Riley, K. Siwek, J. A. Tostevin, and D. Weisshaar, Phys. Rev. C 77 (2008) 044306.
- [17] R. B. Firestone, Nucl. Data Sheets 108 (2007) 1.
- [18] R. G. Thomas, Phys. Rev. 88 (1952) 1109.
- [19] B. A. Brown and W. A. Richter, Phys. Rev. C 76 (2006) 034315.
- [20] R. B. Firestone, Nucl. Data Sheets 106 (2005) 1.
- [21] A. Gade, P. Adrich, D. Bazin, M. D. Bowen, B. A. Brown, C. M. Campbell, J. M. Cook, T. Glasmacher, K. Hosier, S. McDaniel, D. McGlinchery, A. Obertelli, L. A. Riley, K. Siwek, J. A. Tostevin, and D. Weisshaar, Phys. Rev. C 76 (2007) 061302(R).
- [22] I.J. Thompson, Computer code FRESKO. Available at <http://www.fresco.org.uk/index.htm>. See also, I.J. Thompson, Comp. Phys. Rep. 7 (1988) 167.
- [23] J.A. Tostevin, G. Podolyák, B.A. Brown and P.G. Hansen, Phys. Rev. C 70 (2004) 064602; J.A. Tostevin, B.A. Brown, Phys. Rev. C 74 (2006) 064604.
- [24] S. Raman, C.H. Malarkey, W.T. Milner, C.W. Nestor, jr., P.H. Stelson, At. Data Nucl. Data Tables 36 (1987) 1.
- [25] R.W. Wiringa *et al.*, private communication. The configuration and momentum space overlaps are available at <http://www.phy.anl.gov/theory/research/overlap/>